

The effect of titanium alkoxides in the synthesis of heterobimetallic complexes by titanocene(III) alkoxide-induced metal–metal bond cleavage of metal carbonyl dimers

Shota Niibayashi, Kaoru Mitsui, Yukihiro Motoyama, Hideo Nagashima *

Institute for Materials Chemistry and Engineering, Graduate School of Engineering Sciences, Kyushu University, Kasugakouen 6-1, Kasuga, Fukuoka 816-8580, Japan

Received 8 July 2004; accepted 14 September 2004

Abstract

A series of titanocene(III) alkoxides $L_2Ti(III)OR$ where $L = Cp$, $R = Et$ (**1b**), tBu (**1a**), 2,6- $Me_2C_6H_3$ (**1c**), 2,6- $tBu_2-4-Me-C_6H_2$ (**1d**), or $L = Cp^*$, $R = Me$ (**2e**), tBu (**2a**), Ph (**2f**) was synthesized and subjected to reaction with $[CpM(CO)_3]_2$ [$M = Mo, W$], $[CpRu(CO)_2]_2$, and $Co_2(CO)_8$. The Ti(III) precursors **1a**, **1c**, **2a**, **2e**, and **2f** reacted with $[CpM(CO)_3]_2$ [$M = Mo, W$] to form heterobimetallic complexes $L_2Ti(OR)(\mu-OC)(CO)_2MCp$ [$M = Mo, W$], of which Ti and M are linked by an isocarbonyl bridge. Reactions of these Ti(III) complexes with $Co_2(CO)_8$ resulted in formation of Ti–Co₁ heterobimetallic complexes, $Cp_2^+Ti(O^tBu)(\mu-OC)Co(CO)_3$ from **2a**, **2e**, or **2f**, or Ti–Co₃ tetrametallic complexes, $Cp_2Ti(O^tBu)(\mu-OC)Co_3(CO)_9$ from **1a**, **1b**, or **1c**. The products were characterized by NMR, IR, and X-ray crystallography. Reaction mechanisms were proposed from these results, in particular, from steric/electronic effects of titanium alkoxides.

© 2004 Elsevier B.V. All rights reserved.

Keywords: Heterobimetallic complexes; Ti(III) alkoxides; Ti(III) complex; Dinuclear metal carbonyls

1. Introduction

Heterobimetallic complexes have received considerable attention from organometallic chemists in terms of potential cooperative effects by two metals in the complex leading to activation of organic molecules in homogeneous catalysis [1]. In typical examples, their catalysis has been investigated in hydroformylation [2–5], carbonylation [6], hydrogenation/isomerization [7], asymmetric synthesis [8–11], olefin metathesis [12], enol ester formation [13], and olefin polymerization [14]. In our previous papers, we have reported unique access to heterobimetallic complexes by reactions of titanocene

t-butoxides, $Cp_2Ti(O^tBu)$ ($Cp = \eta^5-C_5H_5$; **1a**) and $Cp_2^+Ti(O^tBu)$ ($Cp^* = \eta^5-C_5Me_5$; **2a**), with certain metal carbonyl dimers, $[CpM(CO)_3]_2$ [$M = Mo, W$], $[CpRu(CO)_2]_2$, and $Co_2(CO)_8$ [15]. Heterobimetallic complexes, in which two organometallic units are linked by an isocarbonyl bridge, $Cp_2Ti(O^tBu)(\mu-OC)(CO)_2MCp$ [$M = Mo$ (**3a-Mo**), W (**3a-W**)] and their Cp_2^+Ti -homologues [$M = Mo$ (**4a-Mo**), W (**4a-W**)], were prepared from **1a** or **2a** with $[CpM(CO)_3]_2$, whereas a Ti–Ru complex having a Ti–Ru direct bond, $Cp_2Ti(O^tBu)Ru(CO)_2Cp$ (**5a**), was formed by photo-assisted reaction of **1a** with $[Cp_2Ru(CO)_2]_2$ [15a]. Two Ti–Co complexes, $Cp_2Ti(O^tBu)(\mu-OC)Co(CO)_3$ (**6a**) and $Cp_2^+Ti(O^tBu)(\mu-OC)Co(CO)_3$ (**7a**) were obtained by treatment of **1a** or **1b** with $Co_2(CO)_8$; **6a** readily reacted with $Co_2(CO)_8$ existing in the reaction medium to result in formation of $Cp_2Ti(O^tBu)(\mu-OC)Co_3(CO)_9$ (**8a**) [15b].

* Corresponding author. Tel.: +81925837819; fax: +81925837819.
E-mail address: niba@cm.kyushu-u.ac.jp (S. Niibayashi).

A unique feature of these reactions is that the titanocene(III) *t*-butoxides are good reagents to cleave the metal–metal bond of metal carbonyl dimers, presumably via electron transfer from Ti(III) to the metal dimer, and the metal–metal bond cleavage leads to change of the oxidation state of titanium from III to IV and formation of heterobimetallic complexes. Although formation of anionic organometallic compounds is often seen in reactions of metal–carbonyl dimers with alkali metals or mercury by way of the metal–metal bond fission [16], it is rare that titanium(III) complexes act as reducing reagents. On the other hand, a number of heterobimetallic complexes which have an organotitanium moiety and a metal carbonyl fragment in the molecule have been synthesized and characterized; however, they are commonly synthesized from Ti(IV) precursors [1e,17–21]. In typical examples, treatment of Cp_2TiCl_2 with Li $[\text{Co}_3(\text{CO})_{10}]$ gives $\text{Cp}_2\text{Ti}[(\mu\text{-OC})\text{Co}_3(\text{CO})_9]_2$ and LiCl [17], whereas reaction of Cp_2TiMe_2 with $\text{CpMo}(\text{CO})_3\text{H}$ affords $\text{Cp}_2\text{TiMe}(\mu\text{-OC})(\text{CO})_2\text{MoCp}$ via methane elimination [18]. The closest example to the $\text{Cp}_2\text{Ti}(\text{O}^t\text{Bu})$ -induced heterobimetallic formation is a brief comment from a research group of Moïse, in which reaction of Cp_2TiCl with $\text{Co}_2(\text{CO})_8$ slowly produced $\text{Cp}_2\text{TiCl}(\mu\text{-OC})\text{Co}_3(\text{CO})_9$ [22]. We reexamined the reaction of Cp_2TiCl with $\text{Co}_2(\text{CO})_8$ and compared its reaction rate with the reaction of **1a** with $\text{Co}_2(\text{CO})_8$ under similar conditions; The reaction of Cp_2TiCl was approximately 150 times slower than that of **1a**. This clearly demonstrates the special reactivity of titanocene *t*-butoxides for the heterobimetallic formation, and prompted us to compare their reactivity with other titanocene(III) alkoxides. In this paper, we wish to report our studies and findings on this *t*-butoxide effect, in which a series of titanocene(III) alkoxides shown in Fig. 1 were synthesized and systematically reacted with metal carbonyl dimers as shown in Scheme 1. The results showed that two factors, steric circumstance around the titanium center and monomeric or dimeric structure of the titanocene(III) alkoxides, proved to be important.

2. Results and discussion

2.1. Preparation and characterization of titanocene(III) alkoxides

It is known that Cp_2TiCl exists as a chloro-bridged dimer, $\text{Cp}_2\text{Ti}(\mu\text{-Cl})_2\text{TiCp}_2$ [23]. In sharp contrast, the molecular structure of $\text{Cp}_2\text{TiO}^t\text{Bu}$ (**1a**) revealed a monomeric structure as reported previously [15a]. In several other titanocene(III) alkoxides synthesized and characterized, whether the complex is monomeric or dimeric depends on the steric bulkiness of the ligands around the titanium center [24,25]. In fact, a titanocene(III) complex with a small alkoxide ligand such as Cp_2TiOEt (**1b**) is dimeric [24], whereas a sterically bulky titanium alkoxide like $\text{Cp}_2\text{Ti}[\text{O}(2,6\text{-}^t\text{Bu}_2\text{-4-MeC}_6\text{H}_2)]$ (**1d**) exists as a monomer [25]. Since the bulky pentamethylcyclopentadienyl group prevents the dimerization of $\text{Cp}_2^*\text{Ti}(\text{OR})$, **2a**, **2e**, and **2f** are monomeric regardless of the steric bulkiness of the alkoxide [26].

We are interested in a new complex, $\text{Cp}_2\text{Ti}[\text{O}(2,6\text{-Me}_2\text{C}_6\text{H}_3)]$ (**1c**) which has a phenoxide of medium size, and possibly has both monomeric and dimeric structures. Preparation of **1c** was made by treatment of Cp_2TiCl with $\text{Li}[\text{O}(2,6\text{-Me}_2\text{C}_6\text{H}_3)]$ in THF at room temperature for 12 h. Purification of the reaction mixture by sublimation gave **1c** as red violet crystals in 67% yield; these were paramagnetic and showed an ESR signal at $g = 1.98$ in a 1×10^{-5} M toluene solution. The molecular structure of **1c** was determined by crystallography, and the ORTEP view is illustrated in Fig. 2. Similar to the structure of **1a**, **1c** is monomeric, and two Cp and one alkoxide are bound to the titanium center. There are interesting differences in the Ti–O–C bond angle and the bond distances of the Ti–O and O–C bonds in **1c** from those in **1a**: the Ti–O–C angle of **1c** [144.2 (2)°] is smaller than that of **1a** [175 (1)°]. The Ti–O bond of **1c** [1.895 (2) Å] is longer than that of **1a** [1.810 (3) Å], whereas the O–C bond of **1c** [1.343 (4) Å] is shorter than that of **1a** [1.411 (5) Å]. The reason for these significant

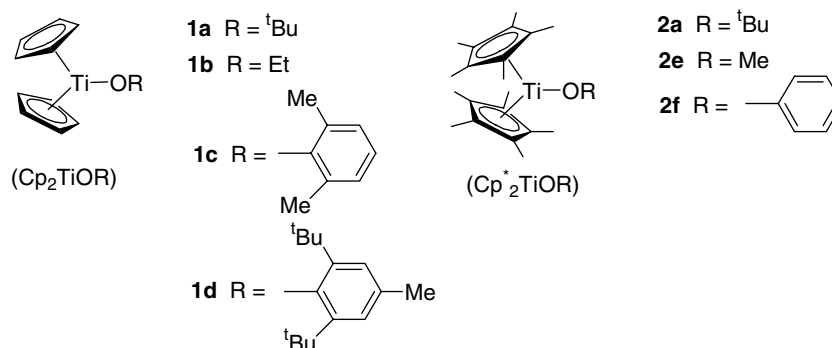
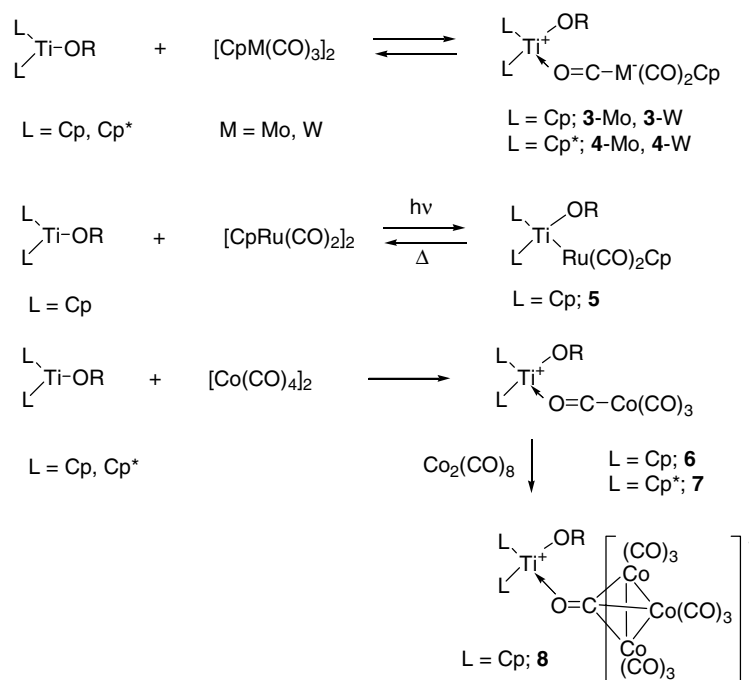
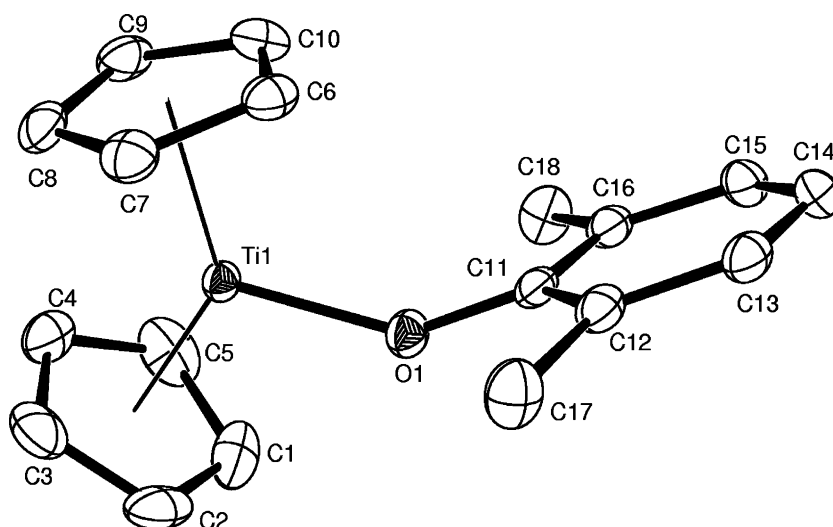


Fig. 1. Titanocene(III) alkoxides.



Scheme 1. The reactions of titanocene(III) alkoxides with metal carbonyl dimers leading to synthesis of heterometallic complexes.

Fig. 2. The ORTEP drawing of **1c**. Thermal ellipsoids are drawn at the 50% probability level. Representative bond distances (Å) and angles (°): Ti(1)–O(1) 1.895(2), O(1)–C(11) 1.343(4), Ti(1)–center of Cp (average) 2.349(1), Ti(1)–O(1)–C(11) 144.2(2), O(1)–Ti(1)–center of Cp (average) 107.4°.

differences in the bond distances and angles can be attributed to the lower electron donating property of the aryl group than the *t*-butyl group. In fact, the angle and bond distances of **1c** are similar to those of another titanocene aryloxy **1d** [25]. As shown in Fig. 3, two lone pairs of the oxygen atom in **1a** have strong interaction with a Lewis acidic titanium center; this makes the Ti–O bond shorter and the Ti–O–C angle larger. The aryl group less electron-donating than alkyl groups causes a reduction in the electron density of the oxygen atom in **1c**, contributing to elongation of the Ti–O bond and shortening of the O–C bond.

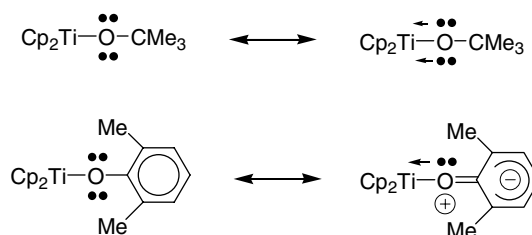


Fig. 3. Two resonance structures for titanocene(III) alkoxides.

We thus obtained the seven titanium(III) alkoxides summarized in Fig. 1, one being dimeric and the other six monomeric, and four the Cp-derivatives, the other three their Cp* analogues. Using these, we next carried out the reactions with metal carbonyl dimers.

2.2. Reactions of titanocene alkoxides with metal carbonyl dimers

First, the titanocene alkoxides synthesized were subjected to the reactions with $[\text{CpMo}(\text{CO})_3]_2$ or $[\text{CpW}(\text{CO})_3]_2$. As reported previously, **1a** and **2a** reacted with $[\text{CpMo}(\text{CO})_3]_2$ or $[\text{CpW}(\text{CO})_3]_2$ to form the corresponding heterobimetallic complex, $\text{Cp}_2\text{Ti}(\text{O}^i\text{Bu})(\mu\text{-OC})(\text{CO})_2\text{MCp}$ [$\text{M} = \text{Mo}$ (**3a-Mo**), W (**3a-W**)] and $\text{Cp}^*\text{Ti}(\text{O}^i\text{Bu})(\mu\text{-OC})(\text{CO})_2\text{MCp}$ [$\text{M} = \text{Mo}$ (**4a-Mo**), W (**4a-W**)] [15]. Among the Cp-substituted titanocene alkoxides, **1b** and **1d** did not react with $[\text{CpM}(\text{CO})_3]_2$, but the reaction with **1c** reversibly formed the corresponding heterobimetallic complexes, **3c-Mo** and **3c-W**; a toluene- d_8 solution of a 1:1 mixture of **1c** and $[\text{CpM}(\text{CO})_3]_2$ gave a 40:60 equilibrium mixture of the heterobimetallic product and the starting materials. Isolation of the complexes was difficult to achieve due to the reversibility of **3c-Mo** or **3c-W** to a mixture of **1c** and $[\text{CpM}(\text{CO})_3]_2$; however, the structures homologous to the *t*-butoxy derivatives can be assigned from the spectroscopic similarities between **3a-Mo** and **3c-Mo** and those between **3a-W** and **3c-W** as summarized in Table 1. In these complexes, ^1H and ^{13}C resonances due to the CpTi and CpM ($\text{M} = \text{Mo}, \text{W}$) moieties are seen in the region of δ_{H} (CpTi) 5.88–5.94, δ_{C} (CpTi) 117.19–118.98, and δ_{H} (CpM) 5.19–5.33, δ_{C} (CpM) 87.81–89.93. Only one ^{13}C signal due to the three CO ligands was visible because of their rapid scrambling in the NMR time scale; however, they can be differentiated by their IR spectra, which showed two terminal (1813–1837 and 1909–1923 cm^{-1}) and one isocarbonyl bridging CO (around 1590 cm^{-1}) absorptions. In other words, the one CO peak observed reflects that cleavage and reformation of the Ti–

OC bond of these complexes were observed by NMR in solution. In the cases of $\text{Cp}_2^*\text{Ti}(\text{OR})$ as starting materials, the reactions were essentially reversible as described later, but the equilibrium was favored for the products. Thus, the products were able to be isolated and completely characterized by spectroscopy as shown in Table 1 and by elemental analysis. Interesting spectral features of these Cp_2^*Ti derivatives of heterobimetallic complexes are three IR absorptions and two ^{13}C resonances due to the CO ligands. This clearly indicates that three CO ligands exist, and two of them are terminal CO and exchangeable in the NMR time scale. The remaining CO ligand is an isocarbonyl bridge, and its Ti–O bond is tight and difficult to dissociate in a C_6D_6 solution.

The reactions of $\text{Co}_2(\text{CO})_8$ took place with all of the titanocene alkoxides except **1d**. Similar to the reactions of **1a**, **1b** and **1c** gave the corresponding Ti– Co_3 products, **8b** and **8c**. The reactions of **2e** and **2f** with $\text{Co}_2(\text{CO})_8$ are analogous to that of **2a** in affording the corresponding Ti–Co complexes, **7e** and **7f**. All of these new compounds are characterized from spectroscopy (Table 2) in comparison with those of **6a**, **7a**, and **8a** reported previously, and the assignments were supported by crystallographic analysis of two of the compounds. The ORTEP drawings of two new compounds, **7e** and **8b**, as well as the representative bond distances and angles are shown in Fig. 4. The heterobimetallic complex **7e** bearing sterically bulky Cp*-ligands has an analogous structure to **7a**. Two metal fragments are linked by an isocarbonyl bridge, and the Ti–O–C–Co moiety is almost linear. Crystallographic disorder problems prevent a detailed comparison in bond distances and angles between **7a** and **7e**, but similarities apparently exist. In contrast, the complex **8b** is a Ti– Co_3 compound analogous to **8a**; the bond length of Ti–O(CCO_3) in **8b** is apparently shorter than **8a** [1.98(1) and 2.026(5) Å, respectively], whereas the C–O bond distance of the isocarbonyl bridge in **8b** is longer than **8a** [1.297(15) and 1.231(7) Å, respectively]. Since the OEt group in **8b** is less bulky than the O^iBu moiety in **8a**, the steric repulsion

Table 1
Spectral data of Ti–Mo or Ti–W heterobimetallic complexes

Spectroscopy	Assignment	3a-Mo	3c-Mo	3a-W	3c-W	4a-Mo	4e-Mo	4f-Mo	4a-W	4e-W	4f-W
^1H NMR ^a δ , ppm	Cp or Cp*Ti	5.91(s)	5.88(s)	5.94(s)	5.90(s)	1.78(s)	1.73(s)	1.74(s)	1.80(s)	1.74(s)	1.76(s)
	CpM	5.29(s)	5.33(s)	5.19(s)	5.20(s)	5.40(s)	5.38(s)	5.43(s)	5.31(s)	5.28(s)	5.33(s)
^{13}C NMR ^a δ , ppm	Cp or Cp*Ti	117.19	118.98	117.08	118.97	13.00	11.83	12.26	13.08	12.10	12.27
						127.50	126.67	128.87	127.35	126.69	128.66
	CpM	89.35	89.93	87.81	88.39	89.16	89.39	89.64	87.60	88.02	88.06
	CO	226.90	226.99	214.25	214.33	233.50	233.34	223.29	223.84	223.90	223.52
IR (KBr) cm^{-1}	ν_{CO}	248.10	242.47			241.34	242.47	241.26	234.47	232.50	234.57
		1920(s)	1923(s)	1909(s)	1920(s)	1923(s)	1911(s)	1926(s)	1911(s)	1910(s)	1922(s)
		1833(s)	1837(s)	1813(s)	1826(s)	1833(s)	1829(s)	1833(s)	1824(s)	1824(s)	1829(s)
		1648(m)	1587(s)	1601(s)	1587(s)	1653(s)	1618(s)	1639(s)	1619(s)	1814(s)	1642(s)
		1612(m)							1620(s)		

^a Measured in toluene- d_8 (for **3**) or benzene- d_6 (for **4**).

Table 2
Spectral data of Ti–Co or Ti–Co₃ heterometallic complexes

Spectroscopy	Assignment	8a	8b	8c	7a	7e	7f
¹ H NMR, ^a δ, ppm	Cp or Cp*Ti	5.93(s)	6.13(s)	5.96(s)	1.65(s)	1.61(s)	1.62(s)
¹³ C NMR, δ, ppm	Cp or Cp*Ti	115.50	117.67	117.35	12.80	11.68	12.26
	CO	203.30	– ^b	203.03	128.44	125.57	– ^c
IR (KBr) cm ⁻¹	ν co	2077(w)	1988(s)	1999(s)	2019(s)	2019(s)	2021(s)
		2028(sh)	1980(s)	1965(s)	1921(s)	1933(sh)	1936(s)
		2015(s)	1405(s)	1441(s)	1766(s)	1919(s)	1920(s)
		2001(s)				1767(s)	1753(s)
		1989(sh)				1750(s)	
		1972 (m)					
		1472(s)					

^a Measured in toluene-d₈ (for **8a** and **8c**) or benzene-d₆ (for **8b**, **7a**, **7e** and **7f**).

^b The signal was not detected because of rapid CO ligand exchange.

^c The peak was overlapped with the solvent signal.

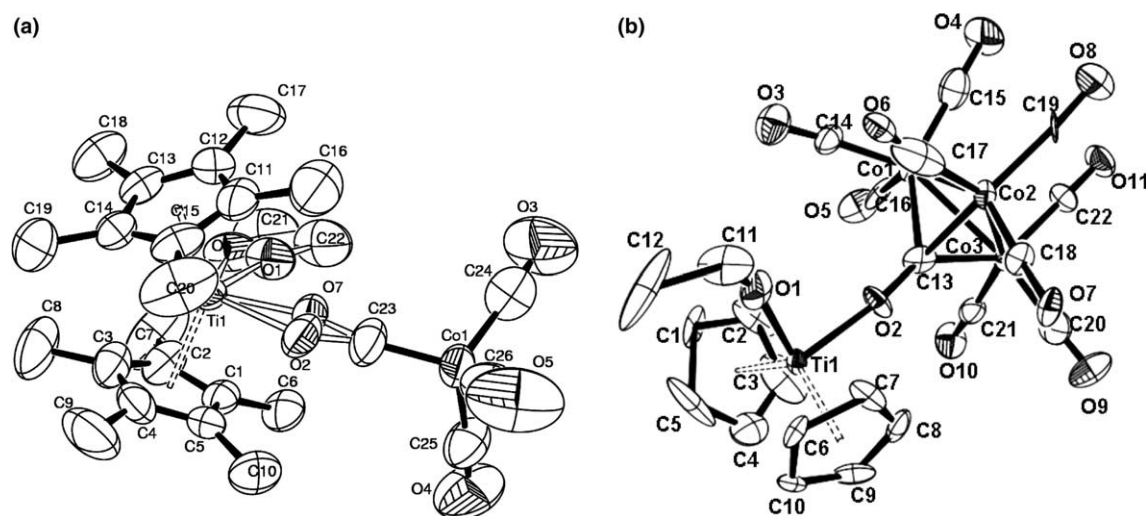


Fig. 4. The ORTEP drawings of (a) **7e** and (b) **8b**. Thermal ellipsoids are drawn at the 50% probability level. Two chemically equivalent but crystallographically independent molecules are included in a unit cell of **8b**, and one of them is illustrated in this figure. Representative bond distances (Å) and angles (°): **7e** Ti(1)–O(2) 2.23(1); O(2)–C(23) 1.26(1); Ti(1)–O(1) 1.813(9); O(1)–C(22) 1.42(2); C(23)–Co(1) 1.686(5); **8b** Ti(1)–O(1) 1.79(1); O(1)–C(11) 1.33(2); Ti(1)–O(2) 1.98(1); O(2)–C(13) 1.29(2); Ti(1)–O(1)–C(11) 151.1(8); Ti(1)–O(2)–C(13) 162.9(10); O(1)–Ti(1)–O(2) 98.2(5).

between the Cp* ring and the alkoxy group is likely to be reduced. We also confirmed the structural analogy of **8c** to **8a** or **8b** by crystallography of **8c**, though the *R* value (*R*₁ = 0.11) was not satisfactory (see [Supporting information](#)). The reactions of [CpRu(CO)₂]₂ with all of the titanocene alkoxides other than **1a** did not occur either thermally or photochemically (see [Table 4](#)).

A summary of these reactions is shown in [Table 3](#). In the reactions of Cp₂TiOR with [CpMo(CO)₃]₂ or [CpW(CO)₃]₂, it is of interest that two of the titanocene(III) alkoxides did not react at all: one is a dimer, [Cp₂Ti(OEt)]₂ (**1b**), whereas the other is Cp₂Ti[O(2,6-*t*Bu₂-4-MeC₆H₂)] (**1d**) having a sterically bulky phenoxide. A monomeric form of **1b** could be generated reversibly in solution; however, its reaction with [CpM(CO)₃]₂ would be less favorable than the re-

verse formation of the dimer. Two *t*Bu groups in the O(2,6-*t*Bu₂-4-MeC₆H₂) group in **1d**, of which the molecular structure was determined by Cetinkaya et al. [25], completely protected the metal center, and prohibited access of the CpM(CO)₃ species to the titanium atom. The heterobimetallic formation proceeded when OR = O^{*t*}Bu and O(2,6-Me₂C₆H₃); the reaction rates are significantly different [OR = O^{*t*}Bu ≫ O(2,6-Me₂C₆H₃)]. The electron-donating *t*BuO group may contribute to the rapid reaction. Three complexes, **2a**, **2e**, and **2f** having electron-rich Cp* ligands also react with [CpM(CO)₃]₂ almost instantly regardless of the alkoxy group (O^{*t*}Bu, OMe, and OPh) attached to the titanium atom. As reported previously, the Ti–Mo and Ti–W heterobimetallic complex formation is essentially reversible [15a]. Introduction of electron-donating substituents is likely

Table 3
Reactions of L₂TiOR with [CpM(CO)₃]₂ (M = Mo, W) or Co₂(CO)₈

L ₂ TiOR	Reaction with [CpMo(CO) ₃] ₂			Reaction with [CpW(CO) ₃] ₂			Reaction with Co ₂ (CO) ₈		
	Time ^a	Product (% yield)	Eq. ^b	Time ^a	Product (% yield)	Eq. ^b	Time ^a	Product (% yield)	Eq. ^b
1a	<5 min	3a-Mo (–)	26:74	<5 min	3a-W (–)	30:70	<5 min	8a (60)	0:100
1b	No reaction			No reaction			48 h	8b (65)	0:100
1c	48 h	3c-Mo (–)	60:40	48 h	3c-W (–)	60:40	48 h	8c (40)	0:100
1d	No reaction			No reaction			No reaction		
2a	<5 min	4a-Mo (70)	0:100	<5 min	4a-W (61)	0:100	<5 min	7a (66)	0:100
2e	<5 min	4e-Mo (42)	0:100	<5 min	4e-W (20)	0:100	<5 min	7e (67)	0:100
2f	<5 min	4f-Mo (70)	0:100	<5 min	4f-W (72)	0:100	<5 min	7f (68)	0:100

^a The reaction time to reach the equilibrium.

^b The equilibrium ratio of the starting materials to the bimetallic product.

Table 4
Crystallographic tables of **1c**, **7e**, and **8b**

	1c	7e	8b ^d
Empirical formula	C ₁₈ H ₁₉ O ₁ Ti	C ₂₅ H ₃₃ O ₅ TiCo	C ₂₂ H ₁₅ O ₁₁ TiCo ₃
Formula weight	299.25	520.34	680.05
Crystal system	Orthorhombic	Triclinic	Triclinic
Space group	<i>P</i> 2 ₁ 2 ₁ 2 ₁	<i>P</i> $\bar{1}$	<i>P</i> 1
<i>a</i> (Å)	7.945(3)	10.6577(12)	8.250(3)
<i>b</i> (Å)	13.831(7)	13.0602(16)	12.481(5)
<i>c</i> (Å)	13.889(6)	9.9219(13)	13.372(5)
α (°)	90	95.247(6)	93.55(3)
β (°)	90	107.642(4)	87.47(3)
γ (°)	90	92.517(6)	112.52(3)
<i>V</i> (Å ³)	1526(1)	1306.8(3)	1269.1(8)
<i>Z</i>	4	2	2
<i>D</i> _{calcd} (Mg/m ³)	1.302	1.322	1.779
Absorption coefficient (μ, mm ^{−1})	0.554	0.970	2.288
<i>F</i> (000)	628	544	676
Crystal size (mm)	0.50 × 0.20 × 0.15	0.45 × 0.35 × 0.05	0.10 × 0.10 × 0.10
Number of reflections measured	3496	5578	9328
Number of independent reflections (<i>R</i> _{int})	3496 (0.00)	5578 (0.00)	9328 (0.00)
Number of reflections observed (>2σ)	3254	3324	7268
Refinement method	Full-matrix least-squares on <i>F</i> ²	Full-matrix least-squares on <i>F</i> ²	Full-matrix least-squares on <i>F</i> ²
GOF ^a	1.068	1.023	1.03
<i>R</i> ₁ [<i>I</i> > 2σ(<i>I</i>)] ^b	0.0505	0.0711	0.0414
<i>wR</i> ₂ [<i>I</i> > 2σ(<i>I</i>)] ^c	0.0568	0.1272	0.0967
<i>R</i> ₁ (all data) ^b	0.1085	0.1577	0.0618
<i>wR</i> ₂ (all data) ^c	0.1109	0.1943	0.1063
Δρ _{max} (e Å ^{−3})	0.466 and −0.608	0.351 and −0.520	0.455 and −0.765

^a GOF = [∑ w(*F*_o² − *F*_c²)/(*N* − *P*)]^{1/2}.

^b *R*(*F*) = ∑ ||*F*_o − *F*_c||/∑ |*F*_o|.

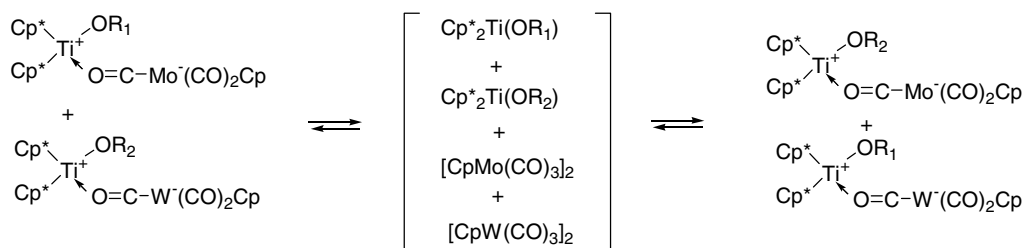
^c *wR*(*F*₂) = [∑ w(*F*_o² − *F*_c²)²/∑ w(*F*_o²)²]^{1/2}.

^d Two chemically equivalent but crystallographically independent molecules are included in a unit cell.

to take part in favorable formation of the product; the equilibrium ratios between the starting materials, L₂Ti(OR) and [CpM(CO)₃]₂, and the product, L₂Ti(OR)(μ-OC)(CO)₂MCp, were altered in the order of electron donating nature of the auxiliary ligands, i.e., 60:40 [L = Cp, OR = O(2,6-Me₂C₆H₃)], 26: 74–30:70 [L = Cp, OR = O^tBu], and 0:100 (L = Cp* regardless of OR). Although the reaction of Cp*₂Ti(OR) with [CpM(CO)₃]₂ looked irreversible, the following NMR experiments offering evidence for the scrambling of the metal fragments as shown in Scheme 2 unequivocally proved the reversibility. Thus, ¹H NMR spectrum of a

mixture of **4e-Mo** and **4f-W** at room temperature gave peaks due to a mixture of **4e-Mo**, **4e-W**, **4f-Mo**, and **4f-W**. Similarly, reaction of **4a-W** with **4f-Mo** took place instantly to afford a mixture of **4a-Mo**, **4a-W**, **4f-Mo**, and **4f-W**.

The titanocene(III) alkoxides reacted with Co₂(CO)₈ to result in formation of the Ti–Co products. Exception is **1d** which is sterically crowded around the titanium atom. Similar to the reactions of the titanocene(III)-*t*-butoxides, **1a** and **2a**, those of Cp₂Ti(OR), **1b** and **1c**, gave the corresponding clusters containing one Ti and three Co atoms, whereas Cp*₂Ti(OR) complexes, **2e**

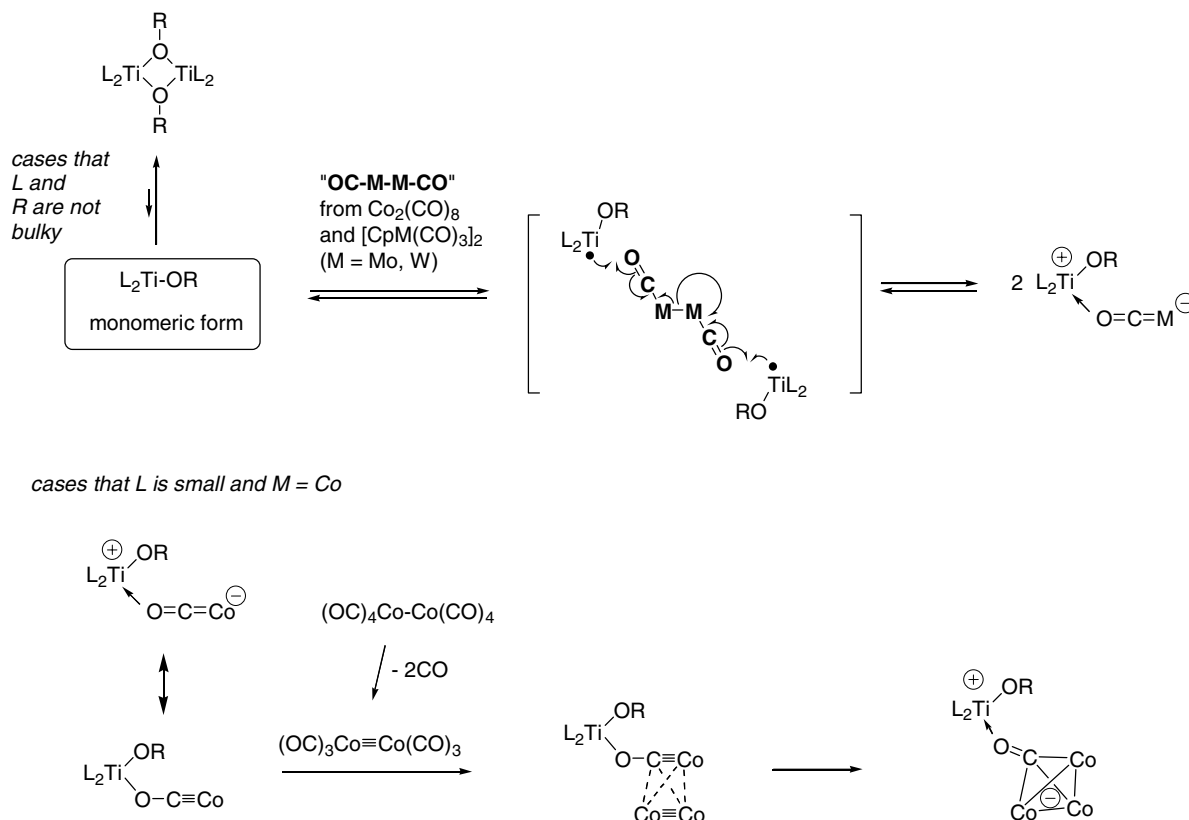


Scheme 2. Scrambling of metal fragments suggesting the reversibility of the reaction of $\text{Cp}^*_2\text{Ti}(\text{OR})$ with $[\text{CpM}(\text{CO})_3]_2$ ($\text{M} = \text{Mo}, \text{W}$).

and **2f**, formed the Ti–Co heterobimetallic products. The reason why Ti–Co₃ clusters formed in the reactions of the Cp-substituted titanocene alkoxydes can be attributed to the fact that the Ti–Co bimetallic complexes are generally not very stable unless the bulky and electron-donating Cp* ligands stabilize them, as discussed in our previous paper [15]. Among the monomeric titanocene alkoxydes, **1a**, **1c**, **2a**, **2e**, and **2f**, **1c** reacted $\text{Co}_2(\text{CO})_8$ more slowly than others; this is attributed to the electron-withdrawing nature of the aryloxy ligand as discussed in the reactions with $[\text{CpM}(\text{CO})_3]_2$. Of particular importance is that $\text{Co}_2(\text{CO})_8$ can react with a monomer, $\text{Cp}_2\text{Ti}(\text{OEt})$, which is reversibly formed the dimer, $[\text{Cp}_2\text{Ti}(\mu\text{-OEt})_2]$ (**1b**), in solution. Since regeneration of the dimer of $\text{Cp}_2\text{Ti}(\text{OEt})$ from the monomer predominantly occurs, the reaction of **1b** with $[\text{CpM}(\text{CO})_3]_2$

does not take place. In contrast, $\text{Co}_2(\text{CO})_8$ is more reactive than $[\text{CpM}(\text{CO})_3]_2$, being reactive with generated monomer to form **8b**. Since this process is somewhat complicated and produces an amount of unknown by-products, detailed analysis of the reaction mechanisms including equilibrium formation of the monomeric form of **1b** is difficult at present. Proposed mechanisms for titanocene(III)-induced reactions with $\text{Co}_2(\text{CO})_8$ or $[\text{CpM}(\text{CO})_3]_2$ are summarized in Scheme 3.

Photo-assisted reaction of titanocene(III) alkoxydes with $[\text{CpRu}(\text{CO})_2]_2$ was only observed when **1a** was used as the organotitanium source. The mechanism must be different from that of the thermal processes shown in Scheme 3, in which electron transfer from the Ti(III) species to the metal carbonyl dimer induces the Ti–O bond formation and the metal–metal bond



Scheme 3. Proposed mechanisms for the titanocene(III) alkoxydes-induced formation of heterobimetallic complexes.

cleavage. One explanation for the photoreaction is generation of $\text{Cp}(\text{OC})_2\text{Ru}^\cdot$, which is trapped by the metal-centered radical of **1a**. The trapping is presumably very sensitive towards a small change of the electronic properties and steric circumstances of the titanium atom, and other titanocene(III) alkoxides shown in this paper are unlikely to be suitable for the Ti–Ru bond formation.

3. Conclusion

The titanocene(III)-induced reactions of metal carbonyl dimers are unique methods for synthesis of heterobimetallic complexes, by which complexes containing one organotitanium moiety and either organomolybdenum, tungsten, ruthenium, or cobalt species are readily obtained. Our previous papers reported special reactivity of titanocene *t*-butoxides, **1a** and **2a**, for these reactions, whereas the present studies changing the alkoxides in $\text{L}_2\text{Ti}(\text{OR})$ (L = Cp or Cp*) clearly demonstrated how electronic and steric factors of the L and OR groups affect the reactions. On the basis of these findings, one can predict the results of the reactions, e.g., the reaction rate, reversibility in the cases using $[\text{CpM}(\text{CO})_3]_2$, and nuclearity of the product in the reaction with $\text{Co}_2(\text{CO})_8$. These results contribute to understanding of the heterobimetallic chemistry, and further synthetic as well as mechanistic studies [27] or these reactions and application of these new complexes to homogeneous catalysis are being undertaken.

4. Experimental

4.1. General

All reactions were carried out with the Schlenk technique associated with experiments using a glove box filled with dry nitrogen gas containing less than 1 ppm of O_2 and H_2O . Toluene- d_8 was dried over sodium and distilled just before use. Other solvents (THF, benzene, toluene, pentane, benzene- d_6) were distilled from sodium benzophenone ketyl, and other reagents were used as received. $[\text{Cp}_2\text{TiCl}]_2$ [28] and titanocene(III) alkoxides, **1a** [15a], **1b** [24], **1d** [25], **2a**, **2e**, and **2f** [26], were prepared according to the methods reported in the literature. NMR spectroscopy was carried out with JEOL Lambda 400 and 600 spectrometers. Chemical shifts (δ , ppm) were recorded from residual peaks of the deuterated solvents. ESR spectra were taken with a JEOL JES FE-3X. IR spectra were measured with a JASCO FT/IR-550 spectrometer and the absorptions were recorded in cm^{-1} . The spectral data of the heterobimetallic complexes are summarized in Tables 1 and 2.

4.2. Preparation of $\text{Cp}_2\text{Ti}[\text{O}(2,6\text{-Me}_2\text{C}_6\text{H}_3)]$ (**1c**)

Preparation of lithium 2,6-dimethylphenoxide was done by treatment of 2,6-dimethylphenol with *n*-BuLi in THF. In a 100 ml flask were placed $[\text{Cp}_2\text{TiCl}]_2$ (213 mg, 0.5 mmol), $\text{Li}[\text{O}(2,6\text{-Me}_2\text{C}_6\text{H}_3)]$ (128 mg, 1 mmol), and THF (30 ml), and the mixture was stirred overnight at room temperature. The resulting red-violet solution was concentrated, and the residue was extracted with toluene (30 ml). After removal of toluene from the extracts, the solid materials were purified with sublimation (2×10^{-2} Torr, 90 °C) to afford the desired product. The solid was recrystallized from THF/pentane to afford purple needle-like crystals of **1c** in 67% yield (200 mg); m.p. 116–117 °C. Anal. Calcd. for $\text{C}_{18}\text{H}_9\text{OTi}$: C, 72.19; H, 6.39. Found: C, 71.92; H, 6.40%. ^1H NMR (C_6D_6) broad peaks appeared at δ 4.13, 4.74, 8.00. MS (m/z) 299. ESR (toluene, 1×10^{-5} M) $g = 1.98$.

4.3. Reversible reactions of $\text{Cp}_2\text{Ti}(\text{OR})$ with $[\text{CpM}(\text{CO})_3]_2$

In a typical example, **1c** (6.0 mg, 0.02 mmol) and $[\text{CpMo}(\text{CO})_3]_2$ (4.9 mg, 0.01 mmol) were dissolved in toluene- d_8 in a 5 mm i.d. NMR tube. The reaction was achieved instantly, and produced an equilibrium mixture of the product (**3c-Mo**) and the starting materials (**1c** and $[\text{CpMo}(\text{CO})_3]_2$) in a ratio of 40:60. In a similar fashion, an equilibrium mixture of **3c-W**, **1c**, and $[\text{CpW}(\text{CO})_3]_2$ was obtained (the product: the starting materials = 40:60). The products were assigned from the spectroscopic similarity to **3a-Mo** or **3a-W** as summarized in Table 1.

4.4. Reactions of $\text{Cp}_2^*\text{Ti}(\text{OR})$ with $[\text{CpM}(\text{CO})_3]_2$

In a typical example, $\text{Cp}_2^*\text{TiOMe}$ (**2e**) (35 mg, 0.10 mmol) and $[\text{CpMo}(\text{CO})_3]_2$ (25 mg, 0.051 mmol) were dissolved in toluene (4 ml) in a 20 ml Schlenk tube. The resulting dark red solution was stirred for 5 min at room temperature. After removal of the solvent in vacuo, the residue was recrystallized from a mixture of THF and pentane to give the desired product, **4e-Mo**, as brown microcrystals (25 mg). NMR observation of the crude product revealed the complete conversion of the starting materials to the product; however, significant loss of the materials in the recrystallization process lowered the isolated yields of the products. **4e-Mo**: 42% isolated yields; m.p. 183 °C (dec). Anal. Calcd. for $\text{C}_{29}\text{H}_{38}\text{O}_4\text{TiMo}$: C, 58.59; H, 6.44. Found: C, 58.55; H, 6.39%. **4e-W**: 20% isolated yields; m.p. 168 °C (dec). Although the equilibrium inhibited the preparation of samples suitable for elemental analysis, its spectroscopic similarity to **4e-Mo** is enough to assign the structure of **4e-W**. **4f-Mo**: 70% isolated yields; m.p. 195 °C (dec). Anal. Calcd. for $\text{C}_{34}\text{H}_{40}\text{O}_4\text{TiMo}$: C,

62.20; H, 6.14. Found: C, 62.12; H, 6.11%. **4f-W**: 72% isolated yields; m.p. 217 °C (dec). Anal. Calcd. for $C_{34}H_{40}O_4TiW$: C, 54.86; H, 5.42. Found: C, 54.88; H, 5.46%. **4a-W**: 61% isolated yields; m.p. 145 °C (dec). Anal. Calcd. for $C_{32}H_{44}O_4TiW$: C, 53.06; H, 6.12. Found: C, 52.86; H, 6.15%.

4.5. Reactions of $Cp_2Ti(OR)$ with $Co_2(CO)_8$

In a typical example, **1c** (60 mg, 0.20 mmol) and $Co_2(CO)_8$ (137 mg, 0.40 mmol) were dissolved in toluene (5 ml) in a 20 ml Schlenk tube. The mixture was stirred in a glove box for two days at room temperature. After removal of the solvent in vacuo, excess amounts of $Co_2(CO)_8$ were removed by sublimation (1×10^{-3} Torr, at room temperature, for 1 day). Recrystallization of the resulting black solids from toluene at -35 °C gave the desired Ti– Co_3 compound, **8c** as black crystals. NMR observation of the crude product revealed the complete conversion of the starting materials to the product; however, significant loss of the materials in the recrystallization process lowered the isolated yields of the products. **8c**: 40% isolated yields; m.p. 128 °C. Anal. Calcd. for $C_{28}H_{19}O_{11}TiCo_3$: C, 44.48; H, 2.53. Found: C, 44.29; H, 2.63%. Treatment of **1b** with $Co_2(CO)_8$ afforded **8b** (65% isolated yield), and some unidentified by-products. Although a single crystal suitable for X-ray analysis was obtained, difficulty in removing small amounts of the by-products prevented preparation of pure samples suitable for elemental analysis.

4.6. Reactions of $Cp_2^*Ti(OR)$ with $Co_2(CO)_8$

In a typical example, a mixture of **2e** (50 mg, 0.14 mmol) and $Co_2(CO)_8$ (25 mg, 0.07 mmol) was dissolved in THF (5 ml) in a 20 ml Schlenk tube. The resulting dark red solution was stirred for 5 min at room temperature. After the solvent was removed in vacuo, the residue was recrystallized from a mixture of pentane and THF at -30 °C to form **7e** as brown crystals. NMR observation of the crude product revealed the complete conversion of the starting materials to the product; however, significant loss of the materials in the recrystallization process lowered the isolated yields of the products. **7e**: 67% yields; m.p. 120 °C (dec). Anal. Calcd. for $C_{25}H_{33}O_5TiCo$: C, 57.31; H, 6.39. Found: C, 57.23; H, 6.37%. **7f**: 68% yield; m.p. 117 °C (dec). Anal. Calcd. for $C_{30}H_{35}O_5TiCo$: C, 61.87; H, 6.06. Found: C, 61.88; H, 6.03%.

4.7. Attempted photochemical reactions of titanocene(III) alkoxides with $[CpRu(CO)_2]_2$

In a typical example, **1c** (4 mg, 0.013 mmol) and $[CpRu(CO)_2]_2$ (3 mg, 0.007 mmol) were dissolved in toluene- d_8 (0.4 ml) in a NMR sample tube. The sample

tube was flame-sealed under reduced pressure, then irradiated for 4 h by 500 W Xe lamp at -10 °C. The reaction was monitored by 1H NMR spectroscopy.

4.8. X-ray data collection and reduction

Single crystals of **1c**, **7e**, and **8b** were grown from THF/pentane. X-ray crystallography was performed on a Rigaku RAXIS RAPID imaging plate diffractometer with graphite monochromated Mo $K\alpha$ radiation ($\lambda = 0.71070$ Å). The data were collected at 123(2) K (**1c** and **8b**) and 173(2) K (**7e**) using ω scan in the θ range of $3.28 \leq \theta \leq 27.48^\circ$ (**1c**) and $2.46 \leq \theta \leq 27.48^\circ$ (**7e**), $3.05 \leq \theta \leq 27.48^\circ$ (**8b**). Data collection and cell refinement were done using ‘MSC/AFC Diffractometer Control’ on a Pentium computer. The structures were solved by direct method (SIR92) [29a] and were refined using full-matrix least squares (SHELXL97) [29b] based on F^2 of all independent reflections measured. The occupancies of each disordered fragment of **7e** were refined with constraints that their sum is 1 (0.52:0.48). All H atoms were located at ideal positions. They were included in the refinement, but restricted to riding on the atom to which they were bonded. Isotropic thermal factors of H atoms were held to 1.2–1.5 times (for methyl groups) U_{eq} of the riding atoms.

Appendix A. Supplementary data

1H NMR charts showing the metal fragment scrambling in the reactions of **4e-Mo** and **4f-W** (Fig. S-5-1) and that of **4a-W** with **4f-Mo** (Fig. S-6-1). Crystallographic data for the structural analyses have been deposited with the Cambridge Crystallographic Data Centre, CCDC Nos. 243161, 243162, 243163 for compounds **1c**, **7e** and **8b**, respectively. Copies of the data can be obtained, free of charge, from The Director CCDC, 12 Union Road, Cambridge, CB2 1EZ, UK (fax: +44 1223 336033 or e-mail: deposit@ccdc.cam.ac.uk). A preliminary X-ray structure of **8c** is described as a supporting information. Supplementary data associated with this article can be found, in the online version, at doi:10.1016/j.jorganchem.2004.09.075.

References

- [1] (a) For reviews on organometallic clusters, see: D.W. Stephan, *Coord. Chem. Rev.* 95 (1989) 41; (b) R.D. Adams, F.A. Cotton (Eds.), *Catalysis by Di- and Polynuclear Metal Cluster Complexes*, Wiley-VCH, New York, 1998; (c) L.A. Braunstein, L.A. Oro, P.R. Raithby (Eds.), *Metal Clusters in Chemistry*, vol. 2, Wiley-VCH, New York, 1999; (d) N. Wheatley, W. Kalck, *Chem. Rev.* 99 (1999) 3379; (e) L.H. Gade, *Angew. Chem. Int. Ed.* 39 (2000) 2658.

- [2] R. Choukroun, D. Gervais, P. Kalck, F. Senocq, *Organometallics* 5 (1986) 67.
- [3] R. Choukroun, D. Gervais, P. Kalck, F. Senocq, *J. Organomet. Chem.* 335 (1987) C9.
- [4] A.M. Trzeciak, J.J. Ziolkowski, R. Choukroun, *J. Mol. Catal. A* 110 (1996) 135.
- [5] B.E. Bosch, I. Brümmer, K. Kunz, G. Erker, R. Fröhlich, S. Kotila, *Organometallics* 19 (2000) 1255.
- [6] V. Mahadevan, Y.D.Y.L. Getzler, G.W. Coates, *Angew. Chem. Int. Ed.* 41 (2002) 2781.
- [7] M.J. Hostetler, M.D. Butts, R.G. Bergman, *J. Am. Chem. Soc.* 115 (1993) 2743.
- [8] N. Yoshikawa, M. Shibasaki, *Tetrahedron* 57 (2001) 2569.
- [9] M. Shibasaki, H. Sasai, T. Arai, *Angew. Chem. Int. Ed. Eng.* 36 (1997) 1236.
- [10] N. Yoshikawa, Y.M.A. Yamada, J. Das, H. Sasai, M. Shibasaki, *J. Am. Chem. Soc.* 21 (1999) 4168.
- [11] S. Matsunaga, J. Das, J. Roels, E. Vogl, N. Yamamoto, T. Iida, K. Yamaguchi, M. Shibasaki, *J. Am. Chem. Soc.* 122 (2000) 2252.
- [12] P. Le Gendre, M. Picquet, P. Richard, C. Moïse, *J. Organomet. Chem.* 643–644 (2002) 231.
- [13] P. Le Gendre, C. Comte, A. Michelot, C. Moïse, *Inorg. Chim. Acta* 350 (2003) 289.
- [14] Y. Yamaguchi, N. Suzuki, T. Mise, Y. Wakatsuki, *Organometallics* 18 (1999) 996.
- [15] (a) K. Matsubara, S. Niibayashi, H. Nagashima, *Organometallics* 22 (2003) 1376;
(b) S. Niibayashi, K. Mitsui, K. Matsubara, H. Nagashima, *Organometallics* 22 (2003) 4885.
- [16] (a) R.E. Dessy, P.M. Weissman, R.L. Phol, *J. Am. Chem. Soc.* 88 (1966) 5117;
(b) R.B. King, *Acc. Chem. Res.* 3 (1970) 417.
- [17] B. Stutte, V. Batzel, R. Boese, G. Schmid, *Chem. Ber.* 111 (1978) 1603.
- [18] D.M. Hamilton Jr., W.S. Willis, G.D. Stucky, *J. Am. Chem. Soc.* 103 (1981) 4255.
- [19] W.J. Sartain, J.P. Selegue, *J. Am. Chem. Soc.* 107 (1985) 5818.
- [20] C.P. Casey, R.F. Jordan, *J. Am. Chem. Soc.* 105 (1983) 665.
- [21] M.R. Awang, D.R. Barr, M. Green, J.A.K. Howard, T.B. Marder, F.G.A. Stone, *J. Chem. Soc., Dalton Trans.* (1985) 2009.
- [22] J. Martin, M. Fauconet, C. Moïse, *J. Organomet. Chem.* 371 (1989) 87.
- [23] R. Jungst, D. Sekutowski, J. Davis, M. Luly, G. Stucky, *Inorg. Chem.* 16 (1977) 1645.
- [24] E. Samuel, J.F. Harrod, D. Gourier, Y. Dromzee, F. Robert, Y. Jeannin, *Inorg. Chem.* 31 (1992) 3252.
- [25] B. Cetinkaya, P.B. Hitchcock, M.F. Lappert, S. Torroni, J.L. Atwood, W.W.E. Hunter, M.J. Zaworotko, *J. Organomet. Chem.* 188 (1980) C31.
- [26] J.W. Pattiasina, H.J. Heeres, F. Van Bolhuis, A. Meetsma, J.H. Teuben, *Organometallics* 6 (1987) 1004.
- [27] As described earlier [15], reactivity of Cp_2TiO^tBu with metal carbonyl dimers is correlated to the reduction potential of the metal carbonyl dimers measured by cyclic voltammetry. We expected correlation between the oxidation potential of the titanocene(III) alkoxides and their reactivity towards the heterobimetallic complex formation. However, cyclic voltammetric studies of titanocene alkoxides for the determination of their oxidation potentials were hampered; one of the complexes (**2a**) showed a quasi-reversible redox wave, whereas the others gave complicated voltammograms. To seek for the appropriate conditions to look at the redox waves of all of titanocene(III) compounds is under study..
- [28] R.S.P. Coutts, P.C. Wailes, *J. Organomet. Chem.* 47 (1973) 375.
- [29] (a) SIR92: A. Altomare, G. Cascarano, C. Giacovazzo, A. Guagliardi, M. Burla, G. Polidori, M. Camalli, *J. Appl. Crystallogr.* 27 (1994) 435;
(b) G.M. Sheldrick, *SHELXL-97*, 1997.